Pergamon

Int. J. Heat Mass Transfer. Vol. 39, No. 5, pp. 1023–1031, 1996

0017-9310/96 $15.00 + 0.00

0017-9310(95)00191-3

Transient heating and vaporization of a cool dense cloud of droplets in hot supercritical surroundings

TSUNG LEO JIANG

Institute of Aeronautics and Astronautics, National Cheng-kung University, Tainan, Taiwan 70101, Republic of China

and

WEI-TANG CHIANG

National Center for High-performance Computing, P.O. Box 19-136, Hsinchu, Taiwan 30043, Republic of China

(*Received* 8 *July* 1994 *and in final form* 9 *May* 1995)

Abstract—Transient heating and vaporization of cool dense spherical droplet-clouds are studied at supercritical conditions. High-pressure effects are considered for the outer homogeneous and inner heterogeneous flows of the cloud. Numerical results obtained from the present study reveal that droplets in such clouds are less likely to reach the critical mixing state than an isolated single droplet at equivalent supercritical conditions. Heat transfer from the hot surroundings is also less influential at supercritical conditions, resulting in relatively invariant-sized droplet-clouds. For such dense droplet clouds, the D^2-law is invalid at both subcritical and supercritical conditions.

INTRODUCTION

Droplet vaporization and burning in a supercritical pressure environment have been studied extensively in the past decades. These studies are of importance since many practical spray combustion systems, including diesel engines, gas turbine engines and liquid rockets, usually operate at pressures greater than the thermodynamic critical value of injected liquid fuels or oxidizers. The first analysis of transient droplet burning under supercritical conditions was proposed by Spalding [1], and subsequently modified by Rosner [2], where the difficulty of criticality was avoided by assuming a pocket of fuel vapor for the droplet. Supercritical droplet combustion lifetimes were predicted to increase with increasing ambient pressure, since mass diffusion is slower with higher pressures. These results were experimentally confirmed later by Faeth *et al.* [3]. However, a droplet can be represented by a pocket of fuel vapor only when the droplet is immediately heated up to its critical mixing state after being injected into a supercritical environment. As the liquid propellant is injected and atomized at a temperature below its critical value, the droplet can exist as a liquid phase and undergo a subcritical vaporization process with a clear two-phase interface before reaching the critical state. This point has been demonstrated by the later studies for high-pressure single-droplet vaporization [4–8], ignition [9–11], and combustion [12–18]. These research works have made significant contributions towards the understanding of high-pressure effects on single-droplet heating, vaporization and burning processes. Among them, Hsieh *et al.* [5] have carried out a comprehensive numerical analysis of multicomponent single-droplet vaporization under near-critical conditions. They employed a time-dependent formulation for both gas and liquid phases with thermodynamic vapor-liquid phase equilibrium being assumed to exist at the droplet surface. At an ambient temperature of 2000 K and initial droplet diameter and temperature of 100 μm and 300 K, respectively, their results indicated that at a high ambient pressure of 65 atm, the *n*-pentane ($T_c = 469.7$ K) droplet first experiences a short subcritical vaporization process and then reaches its critical mixing state before complete vaporization. Subsequently, Shuen *et al.* [15] extended this work, predicting that at an ambient temperature of 1000 K and ambient pressure above 80 atm, an *n*-pentane droplet under auto-ignition in air also reached the critical mixing state after non-negligible subcritical vaporization.

In practical spray combustion systems, however, single-droplet configuration departs substantially from the reality of nondilute sprays. Experimental observations by Chigier and McGreath [19] showed that droplets in dense sprays vaporized as a group, with the group being surrounded by an external flame zone during vaporization. Yule and Bolado [20] also observed experimentally that an external diffusion flame could be exhibited, enclosing vaporizing drop-

NOMENCLATURE

D	diffusivity [$m^2 s^{-1}$]
h	enthalpy [$J kg^{-1}$]
k	conductivity [$W (m \cdot K)^{-1}$]
P	pressure [$N m^{-2}$]
Q_d	heat demand for droplet heating and vaporization [$W m^{-2}$]
Q_n	heat supply from hot surroundings [$W m^{-2}$]
R_a	radius of the sphere of influence [m]
R_d	droplet radius [m]
R_n	cloud radius [m]
r	radial coordinate [m]
T	temperature [K]
t	time [s]
u	radial gas velocity [$m s^{-1}$]
Y	mass fraction.

Greek symbols

μ	viscosity [$N \cdot s m^{-2}$]
ρ	density [$kg m^{-3}$].

Subscripts

a	sphere-edge condition
dc	droplet center
f	fuel
g	gas phase
i	index of species
n	cloud-edge condition
s	droplet surface
∞	cloud ambient condition.

Superscripts

0	initial condition.

lets for small-droplet sprays. Under such flame configurations, temperature measurements conducted by Khalil and Whitelaw [21] and Kawazoe *et al.* [22] showed that the internal dense region of non-premixed spray is relatively cool with respect to the spray surroundings. Tishkoff [23], using the droplet-in-bubble concept, also showed that the temperature at the droplet ambient region decreased due to heat transferred to the droplet for heating and dilution of the surrounding gas mixture by the relatively cool fuel vapor. Bellan and Cuffel [24] also found that the dilute spray theory substantially over-predicted droplet vaporization rates for fuel-rich sprays, since in the former, the droplet ambient conditions are assumed to be unaffected by vaporization. For uniform, dense clouds of droplets, these authors found [26, 27] that at supercritical pressures, the temperature at the droplet ambient region also decreased substantially. As a result, although 40 μm diameter droplets at an initial ambient temperature of 1250 K and pressure of 60 bar reach the critical mixing state before complete vaporization in dilute sprays, those in dense sprays do not. These spray vaporization studies indicate that the assumption of an infinite surrounding for droplets in dense sprays is non-realistic and the gas mixture around such droplets should be cooler than the hot spray surroundings, resulting from the droplet interaction. Hence, compared to that in dilute sprays, the droplet in dense sprays may undergo a much longer subcritical vaporization process before reaching the critical mixing state.

The studies in [26, 27] were limited to the heterogeneous spray region. The vaporization of a spherical cloud of droplets suddenly immersed in hot nitrogen gas was further studied by these authors [28] to evaluate the mass ejection ratio from the cloud at both subcritical and supercritical conditions, where both the outer homogeneous and inner heterogeneous regions were solved. The initial temperature of the gas mixture in the heterogeneous region was assumed to be as high as that in the spray surroundings. Hence, the heat transfer between the outer homogeneous and the inner heterogeneous regions are very limited. This configuration is useful in investigating the vaporization process of the leading cloud of droplets in a direct fuel-injection engine such as diesel engines. However, as the droplet surroundings are cooled due to the vaporization of the leading cloud of droplets, the subsequent cloud of droplets is injected into a region relatively cooler than the spray surroundings. For this case, the effects of the heat transfer between the homogeneous and heterogeneous regions may become significant because of the marked temperature difference between both regions. The objective of the present paper is thus to investigate how this heat transfer affects the droplet-cloud vaporization, especially at supercritical conditions. This problem is studied through numerical analyses for the transient heating and vaporization processes of a spherical cloud of droplets, which is suddenly immersed in a quiescent relatively cool region with respect to the hot surroundings (see Fig. 1). The transient heat-up process, the cloud expansion (or contraction) process, and the droplet regression process of this initially cool cloud of droplets are examined at both subcritical and supercritical conditions, for both initially large- and small-droplet sprays.

THEORETICAL FORMULATION

The present physical configuration comprises an outer hot homogeneous gas-phase region and an inner cool heterogeneous two-phase region of a spherical cloud of droplets (see Fig. 1). The latter consists of monosized droplets which are uniformly distributed. The radius of the sphere of influence is defined at the half distance between the centers of two adjacent droplets. This sphere radius defines the droplet's ambi-

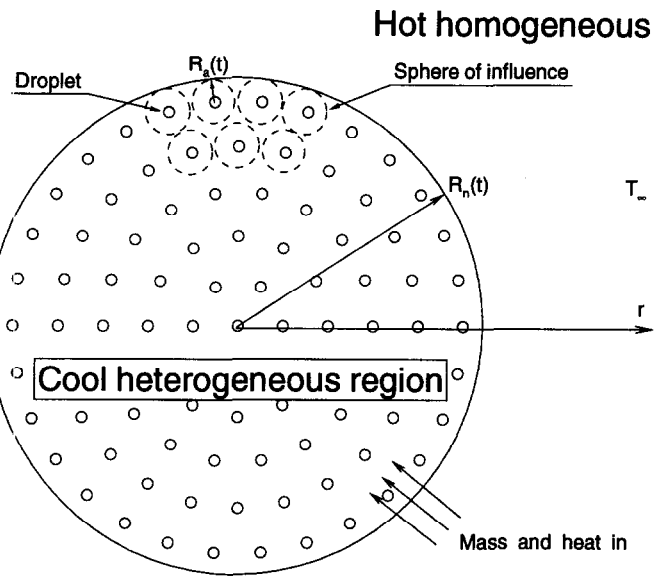

Fig. 1. The configuration and coordinate system for a cool spherical cloud of droplets vaporizing in a hot environment.

ence and varies with time for the present constant-pressure conditions. This configuration, first proposed by Bellan and Cuffel [24], is very useful in accounting for the multi-droplet interaction in sprays. The conditions in the region between the spheres of influence are basically time-dependent and spatially non-uniform. For simplicity, the present study, following Bellan and Cuffel [24], assumes space-uniform properties in that region.

Since the cloud of droplets is assumed to vaporize in a quiescent, zero-gravity environment, forced and natural convective effects are excluded. However, the convective effect associated with the Stefan flow as well as the flow induced by local temperature variations are accounted for through the empirical correlation for the heat transport between the droplet and its surrounding flow. Since this convection effect is not significant, spherical symmetry is assumed for each droplet. Radiation effects and bulk motion in the droplet interior are neglected, and Fick's law is assumed for the species diffusion velocity. The Soret and Dufour effects are also neglected, as they have only limited effects [6].

Three sets of conservation equations are involved for the present problem: (1) global conservation equations for the droplet cloud; (2) governing equations for droplet vaporization within the sphere of influence; and (3) governing equations for the outer gas-flow region. The first set of equations accounts for the transport of mass, fuel species and energy between the outer gas region and the inner two-phase region. The second set of equations involves transient descriptions for both gas and liquid phases within the sphere of influence. Both gas- and liquid-phase equations are solved iteratively such that the gas-droplet interface conditions are satisfied. These interface conditions are based on the conservation of mass and energy, as well as the thermodynamic phase equilibrium assumption. The third set of equations conserves the mass and energy in the outer homogeneous gas-phase region. Therefore, the first set of equations has to be solved based on the results of the second and third sets, and also provides the boundary conditions for both sets of equations. Three sets of equations are thus coupled and have to be solved iteratively. Details of the first and second sets of equations have appeared elsewhere [27, 28]. Governing equations for the outer gas-flow region are given below.

Governing equations for the outer gas-flow region

(a) Mass conservation equation

$$\frac{\partial \rho}{\partial t} + \frac{1}{r^2}\frac{\partial}{\partial r}(r^2 \rho u) = 0. \tag{1}$$

(b) Energy conservation equation

$$\frac{\partial}{\partial t}(\rho h) + \frac{1}{r^2}\frac{\partial}{\partial r}(r^2 \rho u h) = \frac{1}{r^2}\frac{\partial}{\partial r}\left(r^2 k \frac{\partial T}{\partial r}\right) + \frac{1}{r^2}\frac{\partial}{\partial r}\left(r^2 \rho \sum_{i=1}^{N_s} h_{i,g} D_{i,g} \frac{\partial Y_{i,g}}{\partial r}\right) + \tfrac{4}{3}\mu\left(\frac{\partial u}{\partial r}\right)^2 + \tfrac{4}{3}\mu\left(\frac{u}{r}\right)^2 - \tfrac{8}{3}\mu \frac{u}{r}\frac{\partial u}{\partial r}. \tag{2}$$

(c) Species conservation equation

$$\frac{\partial}{\partial t}(\rho Y_{i,g}) + \frac{1}{r^2}\frac{\partial}{\partial r}(r^2 \rho u Y_{i,g}) = \frac{1}{r^2}\frac{\partial}{\partial r}\left(r^2 \rho D_{i,g} \frac{\partial Y_{i,g}}{\partial r}\right). \tag{3}$$

Note that the local gas-mixture density is determined by the use of the equation of state and the mixing rule [26]. The boundary conditions of u, h and

$Y_{i,g}$ at the cloud edge are, however, determined by the global conservation equations for the droplet cloud, while the surrounding conditions are pre-specified. In order to include both pressure and temperature effects on the transport properties of gases and liquids, the appropriate correction formulae, described in [26], are employed.

The governing equations are discretized into their algebraic counterparts based on the finite-volume method and fully implicit scheme [29]. The power-law scheme is used for the convective and diffusive flux over the control volume surface. An effective Newton–Raphson method is developed in solving the interface phase-equilibrium conditions at the droplet surface. For each time-step, rigorous convergence is assured by requiring the maximum residual of the numerical equations smaller than 10^{-5}. In the present analysis, calculations for droplet vaporization are terminated when $(R_d/R_d^0)^2 \leqslant 0.04$.

DISCUSSION OF RESULTS

A dense cloud ($R_a^0/R_d^0 = 5$; $R_n^0 = 1.0$ cm) consisting of *n*-pentane droplets of 300 K suddenly immersed in quiescent, relatively cool nitrogen of 500 K with the latter being heated by the hot surroundings serves as the basis of the present study. The temperature of the hot surroundings is selected at 1000 and 2000 K, respectively. Two initial droplet sizes ($R_d^0 = 20$ and 50 μm) are investigated. The pressure is selected at 5 and 60 bar, representing the subcritical and supercritical conditions, respectively. The critical properties of *n*-pentane and nitrogen are given in refs. [26, 27].

Surrounding temperature effects

In Fig. 2, both the droplet surface and center temperatures are shown with respect to time for a 60 bar pressure. It is interesting to note that for both initial droplet sizes (20 and 50 μm), the droplets never reach the critical mixing state (the critical mixing temperature = 463.1 K) before complete vaporization

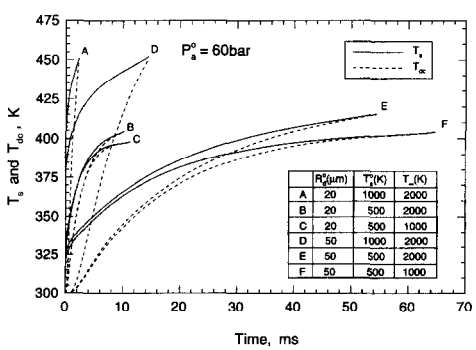

Fig. 2. Variations in the droplet surface and center temperatures over time for two initial droplet-cloud temperatures of 500 and 1000 K and two droplet radii (20 and 50 μm) at a supercritical pressure of 60 bar and two surrounding temperatures of 1000 and 2000 K.

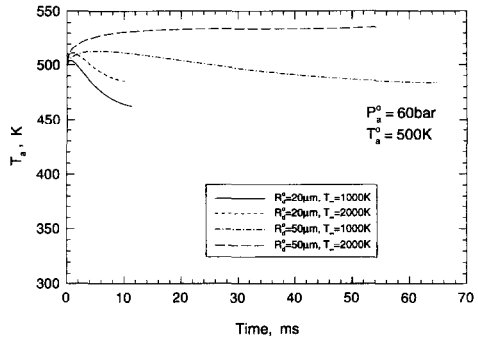

Fig. 3. Variations in the droplet ambient temperature over time for two initial droplet radii (20 and 50 μm) at a supercritical pressure of 60 bar and two surrounding temperatures of 1000 and 2000 K (T_a^0 = 500 K).

even at a supercritical surrounding condition of 60 bar and 2000 K. This result is different from the study of single *n*-pentane droplet vaporization by Hsieh *et al.* [5], where the droplet reaches its critical mixing state before complete vaporization at approximately equivalent supercritical ambient conditions. This difference stems from the fact that as a dense spray is injected into a hot environment, the temperature of the spray interior is initially cool, such as the low temperature of 500 K assumed in the present study other than 2000 K assumed by Hsieh *et al.* [5] for single droplet vaporization. The spray interior remains cool until the droplet depletion, as depicted in Fig. 3, where the temperature in the droplet ambient region is in a narrow range of about 460 and 540 K, only 8% lower and higher than the initial temperature, respectively. As shown in Fig. 4, due to the lower enthalpy of vaporization, the heat supply from the hot surroundings (Q_n) is, in fact, larger than the heat demand for droplet heating and vaporization (Q_d) except for the small-droplet spray with a low 1000 K surrounding temperature. Therefore, the reason that the temperature in the droplet ambient region cannot be quickly raised is mainly because at supercritical conditions, the heat inertia of the gas mixture within

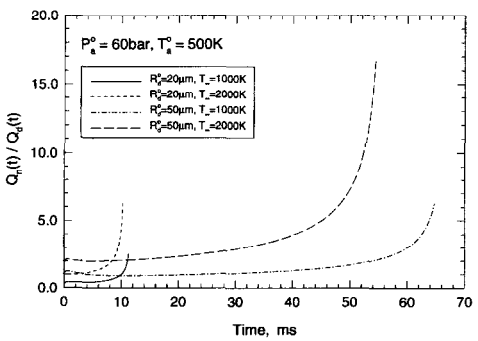

Fig. 4. Variations in the ratio of the heat transfer from the hot surroundings to the droplet cloud to that for droplet heating and vaporization for two initial droplet radii (20 and 50 μm) at a supercritical pressure of 60 bar and two surrounding temperatures of 1000 and 2000 K (T_a^0 = 500 K).

the cloud is large and the droplet lifetime is short. As a result, effects of the surrounding temperature on the heat-up of the droplet cloud are rather limited at supercritical pressures. As depicted in Fig. 2, different surrounding temperatures (1000 and 2000 K) yield little difference in the variations of the droplet surface and center temperatures initially. This effect becomes slightly important only in the final stage of the droplet lifetime, when the energy transferred from the hot surroundings to the droplet cloud becomes huge compared to that for droplet heating and vaporization (Fig. 4). If the initial droplet-cloud temperature is higher such as 1000 K, droplet lifetimes are shown to be much shorter and the droplet surface and center temperatures much higher (Fig. 2). It is thus concluded that at supercritical conditions, the initial temperature in the droplet ambient region is, in fact, much more important than the cloud surrounding temperature for droplet heating and vaporization. Moreover, as depicted in Fig. 2, the droplet heating at supercritical conditions is totally transient, especially for small droplets, as exhibited by the continuously increased droplet surface and center temperatures. The droplet approaches a uniform temperature only in the very final stage of the droplet lifetime when the droplet becomes very small. This is very different from the low pressure case (5 bar; Fig. 5), where the droplet reaches a uniform temperature after a short initial transient period. Therefore, although the quasi-steady droplet vaporization theory, assuming a uniform droplet temperature, is suitable for low-pressure vaporization, it is inadequate for high-pressure vaporization.

After the initial increase due to the fast heat transfer from the hot surroundings, the temperature in the droplet ambient region decreases over time for most of the investigated cases (see Figs. 3 and 6). This is because of the decrease in the specific gas-mixture enthalpy via mixing of the cool fuel vapor. For the large-droplet cloud at 60 bar pressure and 2000 K surrounding temperature, since less energy is demanded because of lower total vaporization rate

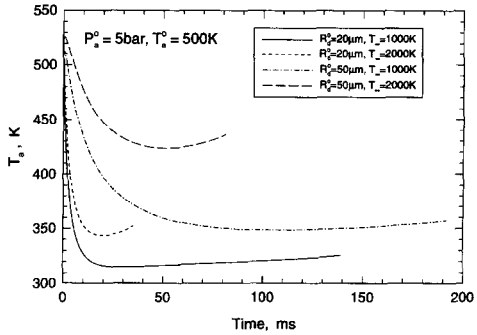

Fig. 6. Variations in the droplet ambient temperature over time for two initial droplet radii (20 and 50 μm) at a subcritical pressure of 5 bar and two surrounding temperatures of 1000 and 2000 K (T_a^0 = 500 K).

and lower enthalpy of vaporization, this cooling effect is countered by the larger energy supply from the hot surroundings. Hence, the temperature increases monotonically. In the final stage of the droplet lifetime, the low-pressure clouds also exhibit an increase in temperature, since the heat supply (Q_n) is substantially larger than the heat demand (Q_d) (see Fig. 7) due to the lower total evaporation rate of becoming smaller droplets. The temperature variations in the droplet ambient region at 5 bar pressure are also responsible for the variations of the droplet surface temperature which first increases, then decreases slightly, and finally increases with respect to time, in contrast to the monotonic increase at 60 bar pressures. For both low- and high-pressure cases, although the droplet lifetime decreases with increasing surrounding temperature, it is interesting to note that in contrast to the substantial reduction in droplet lifetime at the low pressure (Fig. 6), the reduction in droplet lifetime is very limited at the higher pressure (Fig. 3). These results further illustrate that effects of the cloud surrounding temperature on the heating and vaporization of the droplet cloud at high pressures are not so significant as those at low pressures.

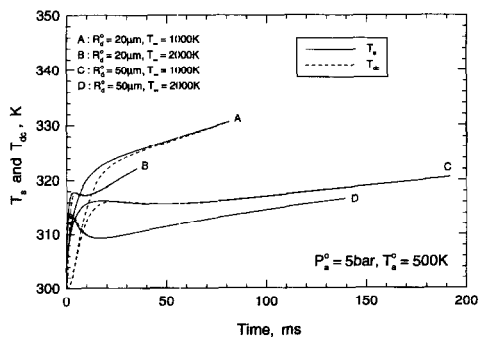

Fig. 5. Variations in the droplet surface and center temperatures over time for two initial droplet-cloud temperatures of 500 and 1000 K and two droplet radii (20 and 50 μm) at a subcritical pressure of 5 bar and two surrounding temperatures of 1000 and 2000 K.

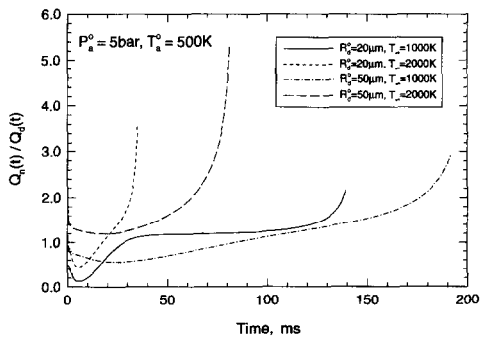

Fig. 7. Variations in the ratio of the heat transfer from the hot surroundings to the droplet cloud to that for droplet heating and vaporization for two initial droplet radii (20 and 50 μm) at a subcritical pressure of 5 bar and two surrounding temperatures of 1000 and 2000 K (T_a^0 = 500 K).

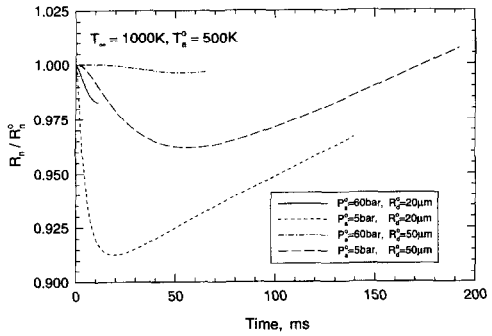

Fig. 8. Variations in the dimensionless droplet-cloud radius for two initial droplet radii (20 and 50 μm) at subcritical (5 bar) and supercritical (60 bar) pressures ($T_\infty = 1000$ K, $T_a^0 = 500$ K).

Drop-cloud size variations

During heating and vaporization processes, the droplet cloud contracts with droplets moving toward the cloud center in balancing the pressure loss due to the temperature drop. It expands with droplets moving outwardly, on the other hand, in suppressing the pressure rise because of the temperature rise and the mass addition by vaporization. At the lower surrounding temperature of 1000 K (Fig. 8), the droplet cloud first contracts and then expands for the lower pressure cases, while it contracts during the whole droplet lifetime for the higher pressure cases. These variations are roughly consistent in trend with the droplet ambient temperature variations (see Figs. 3 and 6). However, it is interesting to note that for the lower pressure cases, after the initial droplet heating period, the increase in droplet-cloud size (Fig. 8) is far more than that in droplet ambient temperature (Fig. 6). This is because the mass-addition effect becomes more significant, making the droplet cloud expand additionally. The mass-addition effect is, however, not significant at the higher pressure due to the lower liquid-to-gas density ratio.

At the higher surrounding temperature of 2000 K (Fig. 9), the smaller-droplet clouds exhibit similar variations in size with those at the lower surrounding temperature (Fig. 8). The larger-droplet clouds, however, expand over time monotonically. This is because the energy supply from the hot surroundings is far more than sufficient to counter the energy loss for droplet heating and vaporization (see Figs. 4 and 7). Therefore, part of the specific enthalpy loss due to the mixing of cool fuel vapor can also be made up by the energy supply. As a result, the mass-addition effect becomes more important than the temperature-drop effect, resulting in more expansion than contraction. Since the mass-addition effect is more significant at the lower pressure due to the higher liquid-to-gas density ratio, the droplet cloud expands to a greater degree. Examination of the expansion (or contraction) ratios for the investigated cases (Figs. 8 and 9) reveals that the droplet cloud at the lower pressure can expand with up to 8% increase in cloud size for the large-droplet (50 μm) cloud at 2000 K and contract with near 9% decrease in cloud size for the small-droplet (20 μm) cloud at 1000 K. Droplet-cloud expansion increases the droplet separation distance, tending to reduce the droplet interaction effect, while droplet-cloud contraction has the opposite influence. At the higher pressure, however, variations of cloud expansion (or contraction) ratios are within 3% and droplet clouds are relatively invariant in size during heating and vaporization processes. Therefore, the effect of droplet-cloud size variations on the droplet interaction is expected to be less significant at the higher pressure.

D^2-Variations

Temporal variations of the square of normalized droplet radius are presented in Figs. 10 and 11 for both the lower and higher pressure cases, respectively. At the lower pressure (Fig. 10), after the initial fast vaporization, vaporization is retarded by the droplet interaction which is evidenced by the temperature and fuel-vapor mass-fraction differences between the droplet surface and ambient region, as shown in Fig. 12. It is especially severe for the smaller-droplet cloud with the lower surrounding temperature, in which the droplet interaction is stronger than that in the other cases. This strong interaction is also evidenced by

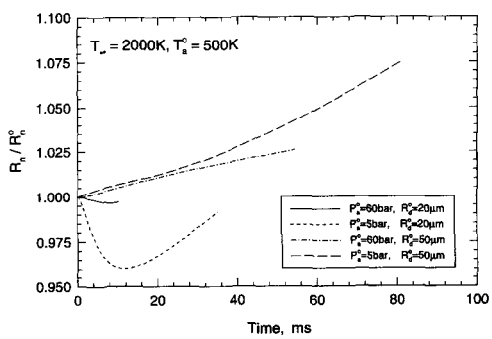

Fig. 9. Variations in the dimensionless droplet-cloud radius for two initial droplet radii (20 and 50 μm) at subcritical (5 bar) and supercritical (60 bar) pressures ($T_\infty = 2000$ K, $T_a^0 = 500$ K).

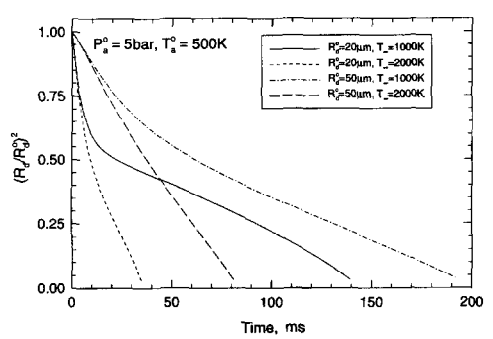

Fig. 10. Variations in the square of normalized droplet radius over time for two initial droplet radii (20 and 50 μm) at a subcritical pressure of 5 bar and two surrounding temperatures of 1000 and 2000 K ($T_a^0 = 500$ K).

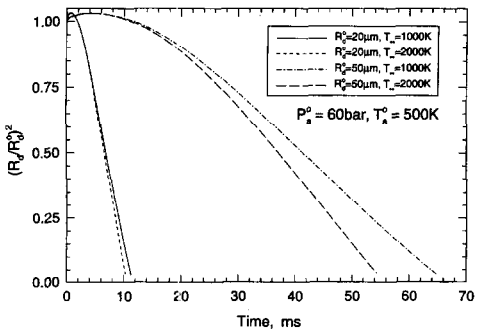

Fig. 11. Variations in the square of normalized droplet radius over time for two initial droplet radii (20 and 50 μm) at a supercritical pressure of 60 bar and two surrounding temperatures of 1000 and 2000 K (T_a^0 = 500 K).

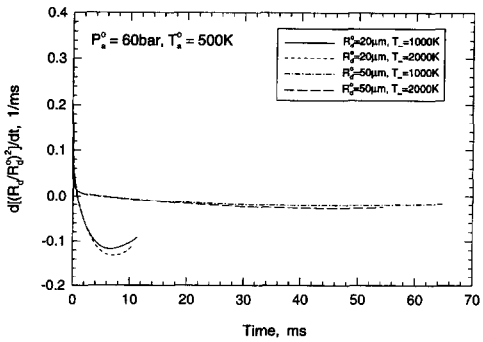

Fig. 13. Variations in the time derivative of the square of droplet radius over time for two initial droplet radii (20 and 50 μm) at a supercritical pressure of 60 bar and two surrounding temperatures of 1000 and 2000 K (T_a^0 = 500 K).

the least fuel-vapor mass-fraction and temperature differences between the droplet surface and ambient region in the final stage of the droplet lifetime (Fig. 12). For droplet vaporization at the lower pressure, the ratio of droplet spatial interval to droplet radius, $R_a(t)/R_d(t)$, increases with regressing droplets. However, the even stronger interaction in the final stage of the droplet lifetime illustrates that for the transient droplet-cloud vaporization, the interaction among droplets does not necessarily lessen with increasing $R_a(t)/R_d(t)$ as quasi-steady analyses suggested. This is because with droplet regression, the droplet-ambient temperature and fuel-vapor mass fraction have also decreased and increased, respectively, both retarding the droplet vaporization. Since the curves in Fig. 10 exhibit marked reflections, the D^2-law is essentially inadequate for the dense cloud of droplets at the lower pressure. Among these lower-pressure cases, the larger-droplet (50 μm) cloud with the higher surrounding temperature (2000 K) follows the D^2-law more closely than the others. This result suggests that the droplet interaction is much weaker for this case, as further evidenced by the largest fuel-vapor mass-fraction and temperature differences between the droplet surface and ambient region (Fig. 12), due to a lower droplet-ambient temperature drop (Fig. 6) and the droplet-cloud expansion (Fig. 9). The latter dilutes the fuel vapor in the gas mixture.

At the higher pressure (Fig. 11), the droplets increase in size initially because of a substantial reduction in liquid density. In this initial period, the droplet is heated up rapidly (see Fig. 2), making a greater increase in liquid volume than decrease in liquid mass. The liquid density may further decrease as the amount of nitrogen dissolved in the droplet becomes significant. After this initial expansion, vaporization of the large-droplet (50 μm) cloud follows the D^2-law closely, especially in the final stage of the droplet lifetime, as depicted by Fig. 13, where the time derivative of the square of normalized droplet radius ($d[(R_d/R_d^0)^2]/dt$) approaches a constant value. This is because the droplet interaction is relatively weaker for the large-droplet cloud, as depicted by the slower increase and decrease in the fuel-vapor mass-fraction and temperature differences, respectively, between the droplet surface and ambient region (see Fig. 14). It should be noted that this result is valid only for the present initially cool droplet-cloud. For an initially hot cloud, the droplet may reach the conditions near the critical mixing state, substantially enhancing the vaporization and making the D^2-law invalid. The

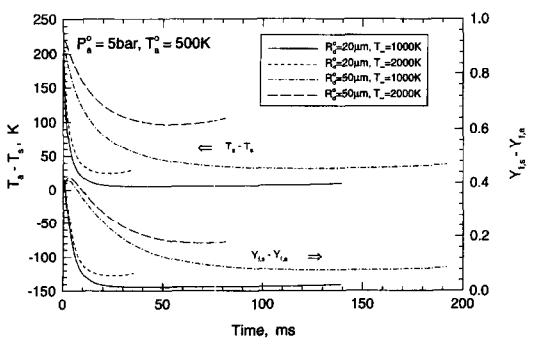

Fig. 12. Variations in the fuel-vapor mass-fraction and temperature differences between the droplet surface and ambient region for two initial droplet radii (20 and 50 μm) at a subcritical pressure of 5 bar and two surrounding temperatures of 1000 and 2000 K (T_a^0 = 500 K).

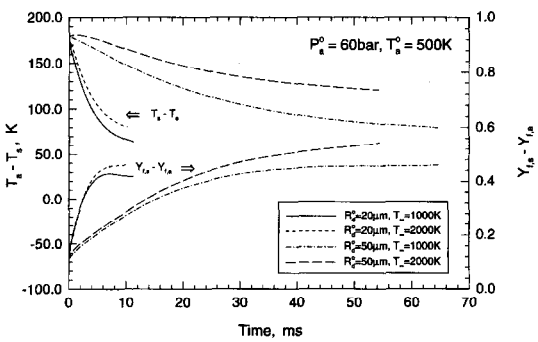

Fig. 14. Variations in the fuel-vapor mass-fraction and temperature differences between the droplet surface and ambient region for two initial droplet radii (20 and 50 μm) at a supercritical pressure of 60 bar and two surrounding temperatures of 1000 and 2000 K (T_a^0 = 500 K).

vaporization of the small-droplet cloud, on the other hand, deviates the D^2-law totally, since the curve for the time derivative of the square of normalized droplet radius never levels off before complete vaporization (Fig. 13). This is due to the fact that the lifetime of small droplets is so short that droplets vaporize completely even before quasi-steady heating is possible (see Fig. 2). It is interesting to note that after the initial droplet-expansion period, $R_a(t)/R_d(t)$ also increases with regressing droplets. However, the effect of droplet regression on the droplet interaction is not so significant as that at the lower pressure, since at the higher pressure, variations in droplet-ambient temperature and fuel-vapor mass fraction, have been very limited during droplet vaporization. This is mainly due to the lower enthalpy of vaporization, higher gas heat-capacity, and higher gas-to-liquid density ratio.

CONCLUSIONS

Heating and vaporization processes of a dense cool cloud of both initially small and large droplets were investigated at supercritical conditions. Transient governing equations for both the inner cool heterogeneous region of a spherical cloud of monosized droplets and the outer hot homogeneous region of gas mixture were solved numerically, with both high-pressure effects and nondilute droplet interaction being taken into account. The following conclusions are drawn from the present study:

(1) At supercritical surrounding conditions, droplets in a dense cloud do not necessarily reach the critical mixing state before complete vaporization as does a single droplet. This is due to the fact that the heat inertia of the gas mixture surrounding droplets is large and the droplet lifetime is short, preventing the droplet ambient region from being heated up by the hot surroundings before the droplet depletes.

(2) With a low ambient temperature of 1000 K, the droplet cloud first contracts and then expands at a 5 bar pressure, while it contracts slightly at a 60 bar pressure. With a high ambient temperature of 2000 K, the large-droplet cloud expands over time monotonically at both the lower and higher pressures. The contraction is due to the heat loss for droplet heating and vaporization. The expansion occurs, however, when the heat loss is countered by the heat supply from the hot surroundings and the mass-addition effect becomes dominant. Due to the higher heat inertia of the gas mixture, the lower liquid-to-gas density ratio and the shorter droplet lifetime, the droplet cloud at supercritical conditions is relatively invariant in size.

(3) Similar to that in an adiabatic droplet cloud [26, 27], the droplet vaporizing in a cool dense cloud with hot supercritical surroundings also exhibits a totally transient heating process. This is especially true for small-droplet clouds. Therefore, the quasi-steady droplet vaporization theory, assuming a uniform droplet temperature, is inadequate for high-pressure vaporization.

(4) For the droplet cloud with the spray density of $R_a^0/R_d^0 = 5$, the D^2-law is invalid at subcritical conditions due to the droplet interaction. It is also inadequate at supercritical conditions in the initial period of the droplet vaporization process due to droplet expansion. After this initial transient period, due to the weak droplet interaction, the D^2-law is suitable for the vaporization of an initially-cool large-droplet cloud, provided that the droplet does not reach the critical mixing state. Vaporization of small-droplet clouds, however, totally deviates from the D^2-law due to the much shorter droplet lifetime.

Acknowledgements—This work was supported by the National Science Council, Taiwan, ROC, under contract NSC 83-0401-E-006-124.

REFERENCES

1. D. B. Spalding, Theory of particle combustion at high pressures, *ARS J.* **29,** 828–835 (1959).
2. D. E. Rosner, On liquid droplet combustion at high pressures, *AIAA J.* **5,** 163–166 (1967).
3. G. M. Faeth, D. P. Dominicis, J. F. Tulpinsky and D. R. Olson, Supercritical bipropellant droplet combustion, *Twelfth International Symposium on Combustion*, pp. 9–18. The Combustion Institute, Pittsburgh (1969).
4. R. L. Matlosz, S. Leipziger and T. P. Torda, Investigation of liquid drop evaporation in a high temperature and high pressure environment, *Int. J. Heat Mass Transfer* **15,** 831–852 (1972).
5. K. C. Hsieh, J. S. Shuen and V. Yang, Droplet vaporization in high-pressure environments, vol I: near critical conditions, *Combust. Sci. Technol.* **76,** 111–132 (1991).
6. E. W. Curtis and P. V. Farrell, A numerical study of high-pressure droplet vaporization, *Combust. Flame* **90,** 85–102 (1992).
7. J. P. Delplanque and W. A. Sirignano, Numerical study of the transient vaporization of an oxygen droplet at sub- and super-critical conditions, *Int. J. Heat Mass Transfer* **36,** 303–314 (1993).
8. H. Jia and G. Gogos, High pressure droplet vaporization; effects of liquid-phase gas solubility, *Int. J. Heat Mass Transfer* **36,** 4419–4431 (1993).
9. T. Kadota, H. Hiroyasu and H. Oya, Spontaneous ignition delay of a fuel droplet in high pressure and high temperature gaseous environments, *Bull. JSME* **19,** 437–445 (1976).
10. R. Ruszalo and W. L. H. Hallett, A model for the autoignition of single liquid droplets at high pressure, *Combust. Sci. Technol.* **86,** 183–197 (1992).
11. R. Ristau, U. Nagel, H. Iglseder, J. Konig, H. J. Rath, H. Normura, M. Kono, M. Tanabe and J. Sato, Theoretical and experimental investigations on droplet evaporation and droplet ignition at high pressures, *Microgravity Sci. Technol.* **6,** 223–228 (1993).
12. D. E. Rosner and W. S. Chang, Transient evaporation and combustion of a fuel droplet near its critical temperature, *Combust. Sci. Technol.* **7,** 145–158 (1973).
13. T. Kadota and H. Hiroyasu, Combustion of a fuel droplet in supercritical gaseous environments, *Eighteenth International Symposium on Combustion*, pp. 275–282. The Combustion Institute, Pittsburgh (1981).
14. J. Sato, M. Tsue, M. Niwa and M. Kono, Effects of natural convection on high-pressure droplet combustion, *Combust. Flame* **82,** 142–150 (1990).

15. J. S. Shuen, V. Yang and C. C. Hsiao, Combustion of liquid-fuel droplets in supercritical conditions, *Combust. Flame* **89,** 299–319 (1992).
16. J. Sato, Studies on droplet evaporation and combustion in high pressures, AIAA Paper 93-0813 (1993).
17. M. Mikami, M. Kono, J. Sato, D. L. Dietrich and F. A. Williams, Combustion of miscible binary-fuel droplets at high pressure under microgravity, *Combust. Sci. Technol.* **90,** 111–123 (1993).
18. T. Tsukamoto and T. Niioka, Numerical simulation of fuel droplet combustion under high pressure, *Microgravity Sci. Technol.* **6,** 219–222 (1993).
19. N. A. Chigier and C. G. McGreath, Combustion of droplets in spray, *Acta Astronaut.* **1,** 687–710 (1974).
20. A. J. Yule and R. Bolado, Fuel spray burning region and initial conditions, *Combust. Flame* **55,** 1–12 (1984).
21. E. E. Khalil and J. H. Whitelaw, Aerodynamic and thermodynamic characteristics of kerosene-spray flames, *Sixteenth International Symposium on Combustion*, pp. 569–576. The Combustion Institute, Pittsburgh (1976).
22. H. Kawazoe, K. Ohsawa and K. Fujikake, LDA measurement of fuel droplet sizes and velocities in a combustion field, *Combust. Flame* **82,** 151–162 (1990).
23. J. M. Tishkoff, A model for the effect of droplet interactions on vaporization, *Int. J. Heat Mass Transfer* **22,** 1407–1415 (1979).
24. J. Bellan and R. Cuffel, A theory of nondilute spray evaporation based upon multiple drop interaction, *Combust. Flame* **51,** 55–67 (1983).
25. K. Harstad and J. Bellan, Electrostatic dispersion of drops in clusters, *Combust. Sci. Technol.* **63,** 169–181 (1989).
26. T. L. Jiang and W. T. Chiang, Effects of multiple droplet interaction on droplet vaporization in subcritical and supercritical pressure environments, *Combust. Flame* **97,** 17–34 (1994).
27. T. L. Jiang and W. T. Chiang, Droplet vaporization in expansible dense sprays at sub- and supercritical conditions, *Atomization Sprays* **4,** 523–549 (1994).
28. T. L. Jiang and W. T. Chiang, Vaporization of a dense spherical cloud of droplets at subcritical and supercritical conditions, *Combust. Flame* **99,** 355–362 (1994).
29. S. V. Patankar, *Numerical Heat Transfer and Fluid Flow* (1st Edn). Hemisphere, Washington, DC (1980).